Commun Nonlinear Sci Numer Simulat 48 (2017) 454–461

Contents lists available at ScienceDirect

Commun Nonlinear Sci Numer Simulat

journal homepage: www.elsevier.com/locate/cnsns

Research paper

Noise induced transitions and topological study of a periodically driven system

Zhen Chen, Xianbin Liu*

State Key Lab of Mechanics and Control for Mechanical Structures, College of Aerospace Engineering, Nanjing University of Aeronautics and Astronautics, 29 YuDao Street, Nanjing 210016, PR China

ARTICLE INFO

Article history:
Received 23 October 2016
Revised 9 January 2017
Accepted 11 January 2017
Available online 12 January 2017

Keywords:
MPEP
Large deviation theory
Lagrangian manifold
Singularities

ABSTRACT

Noise induced transitions of an overdamped periodically driven oscillator are investigated theoretically and numerically in the limit of weak noise due to the Freidlin-Wentzell large deviation theory. Heteroclinic trajectories are found to approach the unstable orbit with fluctuational force tending to zeros. The global minimizer of the action functional corresponds to the most probable escape path and it shows a good agreement with statistical results. We then study the origins of singularities from a topological point of view by considering structures of the Lagrangian manifold and action surface. The switching line and cusp point turn out to have physical significance since they may impact the prehistory distributions, making the optimal path invalid.

1. Introduction

Dynamical systems are often subjected to random perturbations having small amplitudes. However, they may have a profound impact on the dynamics if observations are performed on a sufficient large time scale. For instance, random perturbations result in transitions between various regions around stable states of the deterministic dynamical system, which relates to the so-called metastability observed in a great number of scientific phenomenons, such as chemical reactions, climate regimes, and neuroscience. For small random perturbations, the Freidlin-Wentzel theory[1] of large deviations provides a proper framework to depict their effects on dynamics. Put simply, the theory builds on the fact that almost unlikely events, when they occur, do so with an overwhelming probability in the way that is least improbable. This makes the mechanism of these transitions predictable by using certain action functional which is the central object in the theory. Its minimum serves as the exponential rate of a stationary probability density in the approximated WKB form in the weak noise limit[2] and estimates the transition rates between stable states of the original deterministic system. Moreover, the minimizer of the action functional gives the pathway that is most probable by which the event occurs.

In past decades a great deal of work has been devoted to problems of noise induced transitions or escapes. Smelyanskiy, Dykman and Maier[3] investigated escapes from an unstable focus of a periodically oscillating system. Luchinsky[4] studied the noise driven exit in a double-well system lacking detailed balance and found a bifurcation of MPEPs as parameters varied through analog and digital stochastic simulation. In addition, noise induced escapes from chaotic attractors have also been engaging interest of researchers, such as nonhyperbolic attractors[5,6] and Lorenz attractor[7,8]. Singularities can be observed in the patterns of fluctuational paths, such as cusps and caustics[9–12] since several paths may arrive at the same

* Corresponding author.
E-mail addresses: czkillua@icloud.com (Z. Chen), xbliu@nuaa.edu.cn (X. Liu).

http://dx.doi.org/10.1016/j.cnsns.2017.01.016
1007-5704/

terminal point. However, limited work has been done in the study of topology of Lagrangian manifold and its singularities. Smelyanskiy, Dykman and Maier[3] found the Lagrangian manifold has a novel structure with folds spiraling into the focus. A twisting structure of Lagrangian manifold was demonstrated by studying its separate cross sections along the MPEP and it was found that a birth of a cusp point gave rise to a rotation of the Lagrangian manifold[13]. Dykman[14] studied the fluctuations in a periodically driven overdamped oscillator and briefly discussed the topological properties of the patterns.

In this paper, we continue predecessors' work and investigate the problem from a topological point of view. In contrary to the previous work[11] by the authors, which only considered the fluctuations within the domain of attraction and illustrated some singular features of the pattern, we turn to investigate the noise induced transitions between the metastable states. This phase space is suspended to become $\mathbf{S}^1 \times \mathbf{R}^1$, i.e., the suspension flow is defined on a two dimensional manifold, rather than a plane. Moreover, we try to understand and explain the singular features which are not contained in [11] from a topological point of view, such the cusp point and switching line. The paper is organized as follows. In Section 2, the problem is formulated and the corresponding deterministic system is discussed. In Section 3 the WKB approximation is used. Noise induced escape is then discussed in detail by the method of action plot and several types of escape paths are given. In Section 5 the effect of cusp point and switching line on the escape is considered through the Lagrangian manifold and action surface. Conclusions are drawn in Section 6.

2. Formulation

We investigate an overdamped system driven by a periodic force $K(q; t)$ and white noise $\xi(t)$, the equation of which is

$$\begin{aligned} &\dot{q} = K(q;t) + \xi(t), \quad K(q;t) = K(q;t+T) \\ &\left\langle \xi(t)\xi\left(t'\right)\right\rangle = D\delta\left(t-t'\right) \end{aligned} \tag{1}$$

The model (1) has a wide application in many physical systems and a great deal of effort in its study has been devoted[15–17]. We consider a simple example of model (1) with

$$\dot{q} = -U'(q) + A\cos(\omega t) + \xi(t) \tag{2}$$

$$U(q) = -\frac{1}{2}q^2 + \frac{1}{4}q^4 \tag{3}$$

where A, ω are parameters. The detailed balance condition does not hold due to the presence of external harmonic driving force, with the amplitude A chosen large enough to be beyond the perturbative regime. Only the noise intensity D will be assumed small.

The presence of the external force makes the equilibrium points of the potential U into periodic states, i.e., its two minima become stable periodic cycles and the maximum becomes an unstable cycle. The one-dimensional system (2) is nonautonomous. In order to make it an autonomous system, we have the following

$$\begin{aligned} &\dot{q}_1 = \omega \\ &\dot{q}_2 = -U'(q) + A\cos(q_1) + \xi(t) \end{aligned} \tag{4}$$

The phase space of system (4) is a cylinder defined by $\mathbf{S}^1 \times \mathbf{R}^1$. Fig. 1 shows its vector field for $q_1 \in [0, 2\pi)$, with each arrow denoting the direction of the flow at corresponding point. Three nullclines are also plotted to indicate the periodic orbits, with the middle one unstable and the other two stable. We have set $A = 0.264, \omega = 1.2$ throughout this paper.

3. The WKB approximation

The presence of noise in system (4) may induce transitions from one stable cycle to the other one. If the noise intensity D is small, the escape from the domain of attraction follows a unique optimal trajectory with overwhelming probability, seemingly in an almost deterministic way. To calculate its probability leads us to investigate the asymptotic solution of the corresponding Fokker–Planck equation as $D \to 0$. In the limit of weak noise intensity D one can seek an approximate solution in an eikonal or WKB form

$$P(\mathbf{x}) \sim C(\mathbf{x}) exp[-S(\mathbf{x})/D] \tag{5}$$

with $C(\mathbf{q})$ a prefactor not investigated in this paper and $S(\mathbf{q})$ the activation energy of fluctuations to the vicinity of the point $\mathbf{q} = (q_1, q_2)$ in the state space. $S(\mathbf{q})$ is also called quasipotential or nonequilibrium potential[1].

Substituting Eq. (5) into the Fokker-Planck equation and keeping only the terms of lowest order in D, we acquire the Hamilton–Jacobi equation for $S(\mathbf{q})$:

$$H(\mathbf{q}, \mathbf{p}) \equiv \mathbf{u}(\mathbf{x}) \cdot \mathbf{p} + \frac{1}{2}\mathbf{p}^T\mathbf{p} = 0, \mathbf{p} \equiv \frac{\partial S}{\partial \mathbf{x}} \tag{6}$$

To solve Eq. (6) one can employ the method of characteristics, arriving at the following equations:

$$\frac{d\mathbf{q}}{dt} = \frac{\partial H}{\partial \mathbf{p}} = \mathbf{u}(\mathbf{q}) + \mathbf{p} \tag{7}$$

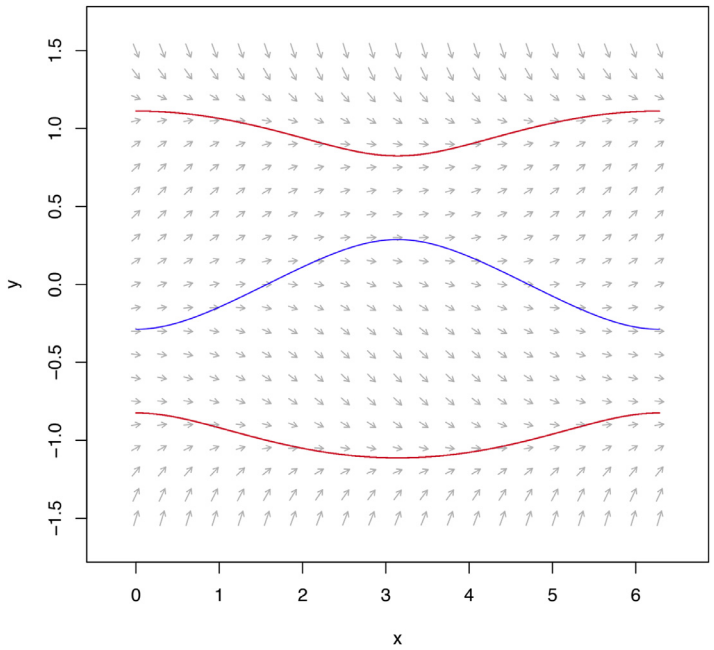

Fig. 1. The vector field of the two dimensional system (4) and nullclines are plotted by blue solid lines. (For interpretation of the references to color in this figure legend, the reader is referred to the web version of this article.)

$$\frac{d\mathbf{p}}{dt} = -\frac{\partial H}{\partial \mathbf{q}} = -\left[\frac{\partial K(\mathbf{q})}{\partial \mathbf{q}}\right]^T \mathbf{p} \tag{8}$$

Note that Eqs. (7) and (8) lead to an auxiliary Hamiltonian dynamical system, with the Wenzel–Freidlin Hamiltonian $H(\mathbf{q}, \mathbf{p})$. From this point of view $S(\mathbf{q})$ can be interpreted as the classical action at zero energy[3].

Solutions of Eqs. (7) and (8) describe trajectories yielding extreme values of the cost functional of the form:

$$S[\mathbf{q}(t)] = \int_{t_0}^{t_f} \xi^2(t)\, dt \tag{9}$$

with $\mathbf{q}(t)$ being certain trajectory driven by corresponding realization of $\xi_i(t)$ and satisfying $\mathbf{q}(t_0) = \mathbf{q}_0$ and $\mathbf{q}(t_f) = \mathbf{q}_f$. Using (4) the cost functional (9) can be transformed into an action functional:

$$S[\mathbf{q}(t)] = \int_{t_0}^{t_f} dt\, L(\mathbf{q}, \dot{\mathbf{q}}), \quad L(\mathbf{q}, \dot{\mathbf{q}}) = \frac{1}{2}(\dot{\mathbf{q}} - \mathbf{u})^T(\dot{\mathbf{q}} - \mathbf{u}) \tag{10}$$

This has the form of a Lagrangian L for a classical mechanical system. As $D \to 0$, these path integrals (10) can be evaluated by means of steepest descents and the paths dominating the integrals are the ones giving rise to $\delta S/\delta \mathbf{q} = 0$. This results in a Euler–Poisson equation for extreme fluctuational paths which is a $2n$th-order nonlinear partial differential equation. It can be converted into 2n first-order ordinary differential equations, which turn out to be Eqs. (7) and (8). In other words, the action $S(\mathbf{q})$ mentioned above is just defined by the variational problem of (10). Combining (4) and (10), we have the Freidlin–Wentzell Hamiltonian for (4) as follows

$$H(\mathbf{q}, \mathbf{p}) = \omega p_1 + \frac{1}{2}p_2^2 + p_2\left(q_2 - q_2^3 + A\cos(q_1)\right) \tag{11}$$

and the auxiliary Hamiltonian system

$$\begin{aligned} \dot{q}_1 &= \omega \\ \dot{q}_2 &= q_2 - q_2^3 + A\cos(q_1) + p_2 \\ \dot{p}_1 &= -A\cos(q_1)p_2 \\ \dot{p}_2 &= -p_2\left(1 - 3q^2\right) \end{aligned} \tag{12}$$

Note that the state space of (12) is $\mathbf{S}^1 \times \mathbf{R}^3$. From the viewpoint of dynamical system, different values of q_1 determine different Poincar cross-sections of system (12), meaning that the paths $(\mathbf{q}(t), \mathbf{p}(t))$ fluctuating to a given point $\left(q_{1f} + 2\pi, q_{2f}\right)$ are the same paths as those to the point (q_{1f}, q_{2f}).

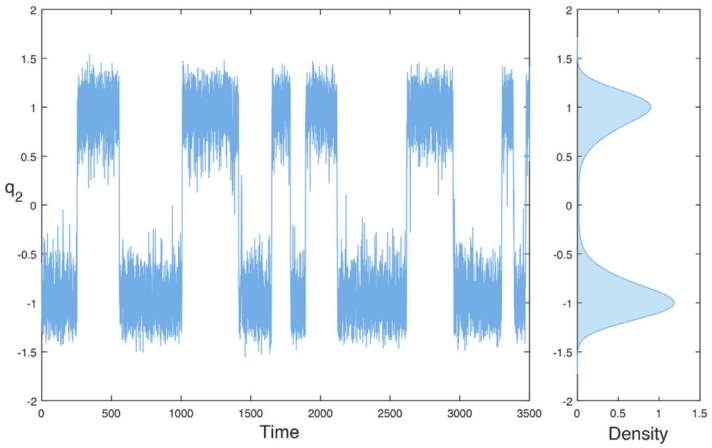

Fig. 2. A realization of system (4) with initial point at $(0, -1)$. The left side shows the time series of q_2 and the right one shows a histogram of q_2 over the entire realization [0, 3500]. We set the noise intensity $D = 0.3$.

4. Noise induced transitions

Now let us turn to investigate noise induced transitions from one stable periodic state to the other. A realization of system (4) driven under noise of intensity $D = 0.3$ is shown in Fig. 2, with a histogram of the state variable during the whole simulating time [0, 3500] on the right side. It can be seen from the density that almost equal amount of time is spent around these two metastable states, suggesting that they have the same stabilities. According to the Freidlin–Wentzell large deviation theory, the mechanism of theses transitions is often predictable for small noise amplitudes. That is to say the transition occurs with overwhelming probabilities by following the most probable escape path (MPEP), which serves as a minimizer to certain action functional (10). Moreover, the knowledge of its minimum allows us to estimate the probability and rate of the rare events.

The method of action plot is then employed to obtain the global minimum of the action functional and the corresponding MPEP. We should note that a transition must occur across the unstable cycle around the maximum of the potential U, composed of an escape from one of the domain of attraction and a relaxation to the other stable cycle. Thus what we mostly concern is the process of noise induced escape. The escaping trajectories from the stable cycle form a one-parameter family on the unstable Lagrangian manifold, which is to be considered in the next section. A possible choice of parametrization can be of the form $(q_1, q_2) = (q_{1c}(\phi), q_{2c}(\phi) + \delta)$, where q_{1c} and q_{2c} are the coordinates of the stable cycle at a given phase ϕ and δ is a small displacement in the q_2 direction. Therefore the phase ϕ is the parameter we use to trace out the set of escape trajectories. We take 10^5 initial points ϕ which are uniformly distributed in $[0, 2\pi)$ and take $\delta = 10^{-4}$ for parametrization. The robustness of this method can be guaranteed if we take the small displacement δ under some lower bound and find no more obvious change in the action plot.

We present the action plot in Fig. 3, exhibiting a rather complicated structure composed of narrow “hills” and very sharp “peaks”. At the edges of each hill local minima of the action can be seen. A zoom inside the dotted box of Fig. 3(a) reveals almost similar structures, see Fig. 3(b). Intuitively, there are two types of escape trajectories. The first type is that they can cross the unstable cycle with nonzero momenta, and move further to enter the other domain of attraction. The second one corresponds to a different scene: they first move towards the unstable cycle but their momenta are not sufficient to escape. Then they are reflected back to the interior of the original basin, fluctuating around the attractor again and preparing for a next trial to escape. Between the two types of escape paths is the third one: heteroclinic trajectories, which approach the unstable cycle on the boundary with momenta tending to zeros. In other words, these heteroclinic trajectories lie on the intersections of the unstable manifold of the attractor and the stable manifold of the saddle, reaching the unstable cycle asymptotically (for $t \to \infty$) and tangentially ($p \to 0$, as $t \to \infty$). We remark that each heteroclinic trajectory corresponds to a discontinuous value in the action plot. In fact, trajectories reflecting back from the basin boundary should carry insufficient momenta in their initial runs. Subsequently they return to the vicinity of the original stable state with momenta nearly zeros since **p** actually measures the deviations from deterministic dynamics, as seen from Eqs. (7) and (10). While preparing the second trials, their momenta will become significantly nonzero again. This results in a highly larger action than that of heteroclinic trajectories. Therefore, the lowest-cost heteroclinic trajectory is the MPEP[3].

The escape trajectory corresponding to the global minimum of the action plot, indicated by a black square in Fig. 3(a), is shown in Fig. 4(a) by a black thick line. It is actually the MPEP from discussions above. As can be clearly seen, the MPEP manifests itself as a heteroclinic trajectory approaching the unstable cycle asymptotically. For an illustration,the momentum of MPEP is denoted by a black thick line in the inner plot, tending to zero as reaching the unstable cycle. Two trajectories of other local minima of the action plot are also given in Fig. 4, corresponding to the arrow-1 and arrow-3 in Fig. 3(b) respectively. Both of them are heteroclinic trajectories with their momenta tending to zero as shown in the inner plot. For

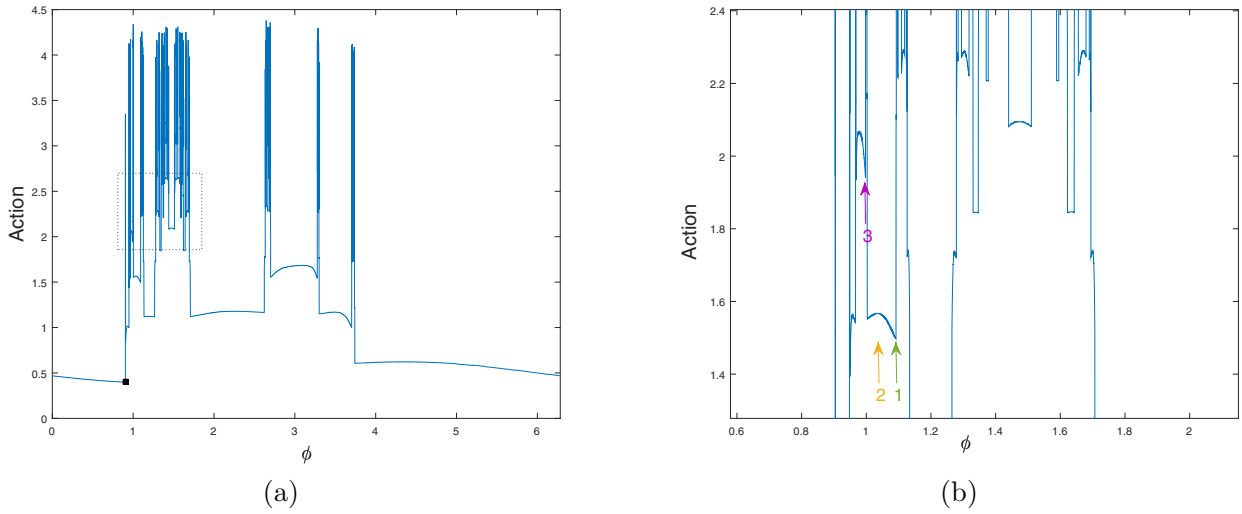

Fig. 3. (a). The action plot. The x axis is the phase ϕ to parameterize the escape trajectories, ranging from $[0, 2\pi)$. The global minimum is indicated by a black filled square. (b). A local amplification of the dotted box in (a). Finer and nested structures are evident and infinite many local minima between each pair of peaks can be seen.

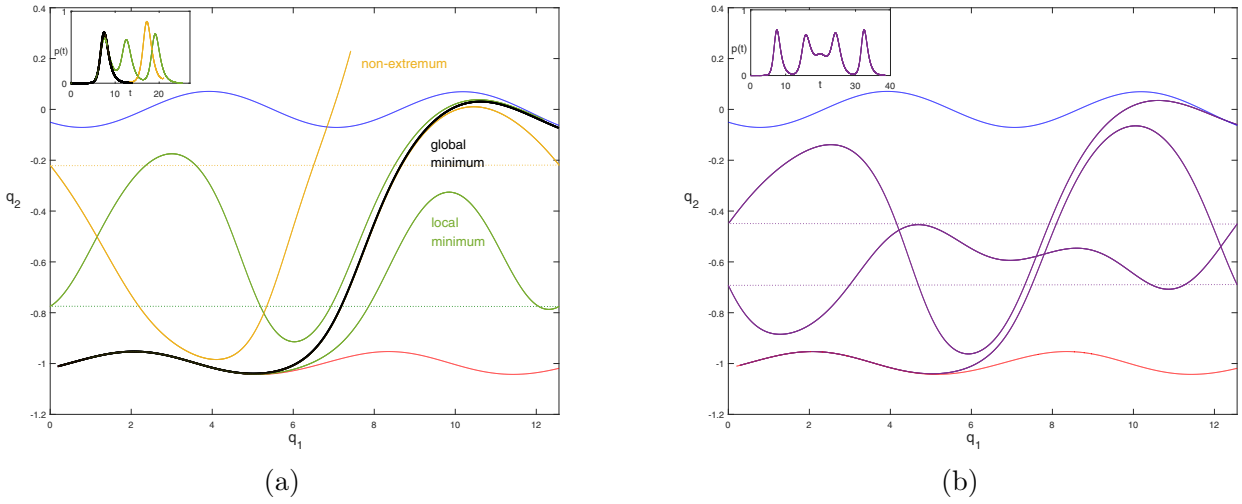

Fig. 4. Escape paths corresponding to the arrows in Fig. 3(b). The red and blue lines denote stable and unstable cycle respectively. The inner plot gives their fluctuational forces.(a).The green thin line for arrow-1, yellow thin line for arrow-2 and the black thick line for MPEP. (b). The purple thin line for arrow-3. (For interpretation of the references to color in this figure legend, the reader is referred to the web version of this article.)

arrow-3 lying on a hill higher than arrow-1, its trajectory experiences an unsuccessful attempt one more time, see Fig. 4(b). This explains the formation of nested structures of the action plot. The trajectory for arrow-2 which lies in the smooth part of the hill, is indicated by a yellow line. Evidently, it finally pierces the unstable cycle with residual momentum. The vary from arrow-2 to arrow-1 is continuous.

Nevertheless, in the limit of small noise intensity, the probability density and the rate of transitions are dominated by the global minimum of the action plot rather than other local ones. This is because contributions of other local minima are exponentially small. Thus in a physical experiment in the zero noise intensity limit only those trajectories of global minima can be observed, as demonstrated in Fig. 5. Numerical results are obtained by means of tracing out peaks of the prehistory probability distribution[18], which turns out to be an appropriate statistical method to describe the distribution of fluctuational paths, both theoretically and experimentally[19]. This distribution contains all the information on the temporal evolution of the system before arriving at the given point, it should peak sharply around the MPEP as $D \to 0$. We set $D = 0.05$ in the numerical simulation and performed an ensemble average of hundreds of escaping realizations. The fluctuational force p_2 during the escape is also simulated by averaging the noise realizations conserved simultaneously with path realizations and performing a low-pass filtering process, denoted by a green zigzag line in Fig. 5(b). The low-pass filtering

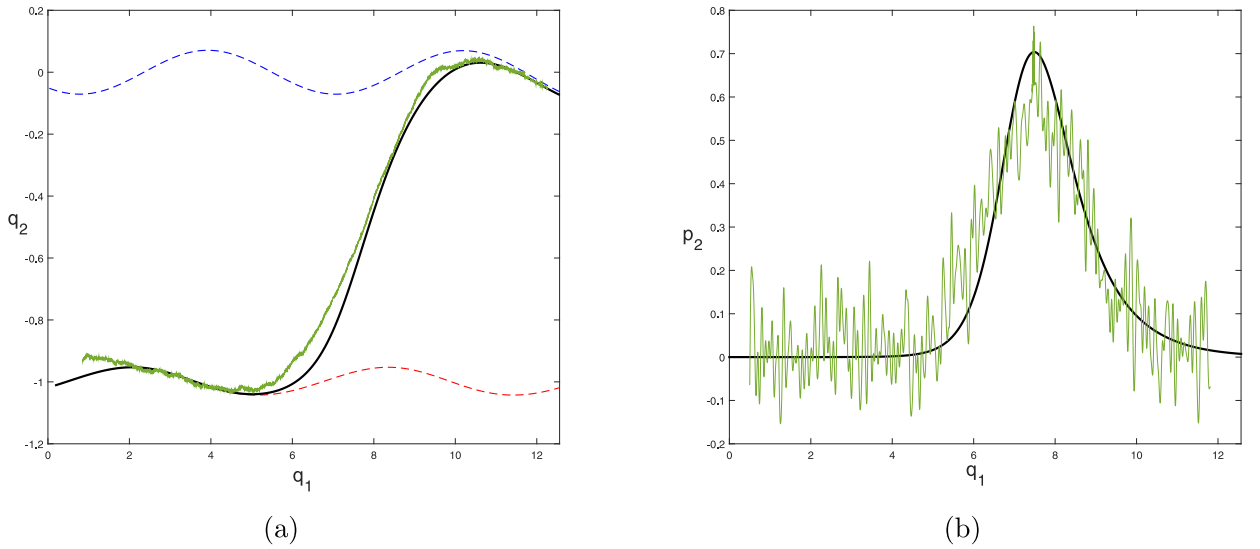

Fig. 5. Comparisons between numerical (green thin lines) and theoretic (black thick lines) results of the MPEP. The red and blue dashed lines denote two stable periodic states respectively. $D = 0.05$. (For interpretation of the references to color in this figure legend, the reader is referred to the web version of this article.)

process helps to reveal the underlying patterns of noises by eliminating their high-frequency components. As can be seen, both results are in good agreements.

5. Topological aspects of singularities

From the last section one can see the existence of multiple local minima of the action functional, which leads to the fact that several fluctuational paths with different parameters ϕ may arrive at the same terminal point $\mathbf{q}$. Thus the actions computed from Eq. (10) will be a multivalued function of the end point, which forms the basic origin of singularities of the pattern of fluctuational paths[11]. In this section we are going to study the singularities from a more topological point of view, by considering the auxiliary Hamiltonian system (12) in its four dimensional phase space. We will see in what cases the concept of most probable paths becomes invalid.

A stable periodic cycle of the deterministic system (4) corresponds to a closed orbit lying on the cylindrical surface $\mathbf{p} = \mathbf{0}$, which is the two dimensional coordinate space (q_1, q_2). The fluctuational trajectories emanating from this limit cycle form a two dimensional Lagrangian manifold. It may have complicated structures so that even though the trajectories never intersect on the manifold, their projections onto the hyperplane $\mathbf{p} = \mathbf{0}$ could exhibit singular patterns. A two dimensional Lagrangian manifold has only two types of singularities which is structurally stable: cusps and folds[20]. Each cusp gives rise to a pair of folds and the projections of folds are caustics. We have plotted the Lagrangian manifold together with the pattern of fluctuational paths in Fig. 6(a), in which the correspondence between folding structures of Lagrangian manifold and the singular region of the pattern is evident.

The Lagrangian manifold has three sheets and the action is thus three valued. It was observed in [11] that trajectories providing the largest value of $S(\mathbf{q})$ trace out the middle sheet of Lagrangian manifold. This sheet is formed by Hamiltonian trajectories that have gone over the folds and in other words, their projections in coordinate space have been reflected by caustics, see Fig. 6(b). It follows that the action functional $S(\mathbf{q})$ must attains its minimum on either the top or bottom sheet. This offers a topological demonstration of the fact that the MPEP never encounters caustics[9].

Generally, different sheets of $S(\mathbf{q})$ will intersect each other transversally, i.e., at a nonzero angle. Along this intersecting curve we have $S^1(\mathbf{q}_f) = S^2(\mathbf{q}_f)$ such that there exists two paths fluctuating to $\mathbf{q}_f$ with almost equal probabilities. They lie on the top and bottom sheets of Lagrangian manifold respectively. Both numerical and theoretical results in such case are given in Fig. 7. It is obvious from Fig. 7(a) that the prehistory probability distribution peaks sharply along two paths drawn above in yellow. Solving the boundary value problem of Eq. (10) through steepest descent method gives three solutions drawn in red, green and cyan lines in Fig. 7(b). On one hand these theoretic solutions fit well in the Lagrangian manifold traced out by Hamiltonian trajectories and on the other hand, numerical results, plotted by yellow lines in Fig. 7(b), are in good agreement with theoretic results. Neither of the two paths turns over a fold and moves into the middle sheet of the Lagrangian manifold as expected.

Paths fluctuating to points that lie a small distance away from the intersecting curve of $S(\mathbf{q})$ but on opposite sides of it are topologically distinguished, as investigated in [11]. It is just why the intersecting curve is referred to as “switching line”, emanating from the cusp point and lying between the coalescing caustics. Recalling the structure of the action surface, in

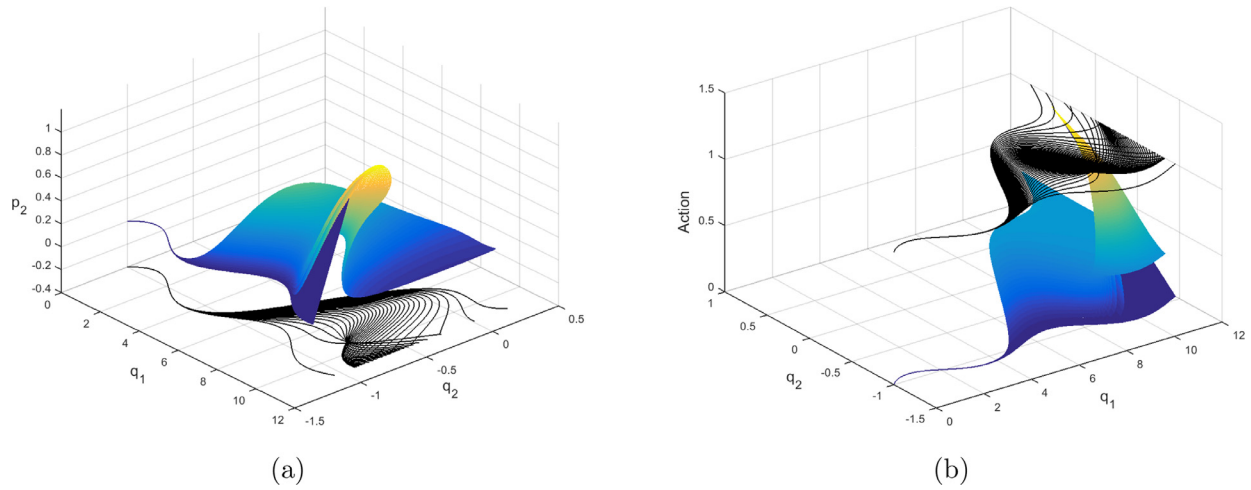

Fig. 6. Lagrangian manifold and action surface emanating from the stable periodic orbit near $q_s = -1$, shown with the pattern of fluctuational paths.

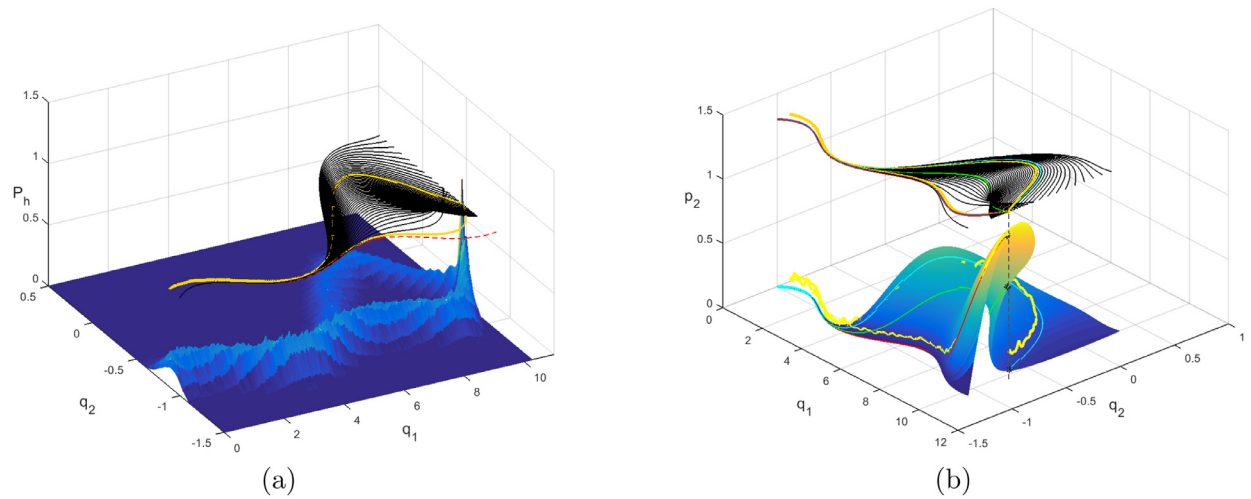

Fig. 7. (a). Prehistory probability distributions peaking along two certain paths plotted above; (b). Solutions of boundary value problems are shown in red, green and cyan lines respectively. The yellow lines are statistical results as in (a). (For interpretation of the references to color in this figure legend, the reader is referred to the web version of this article.)

a close vicinity of the cusp point values of actions on the three sheets are roughly equally. Hence there is a large family of paths fluctuating into this tiny region with nearly the same actions, that is to say, with nearly the same probabilities, yielding extensively broadening of the distribution near the cusp point. One can see Fig. 8 for an illustration: closer to the cusp, broader the distribution. It is just this acute flattening of the distribution that makes the fluctuational paths in physical experiments “less deterministic” in the sense of large deviation theory. Hence if the end point is selected close to the cusp point, the fluctuational paths becomes more random and none of them seems to be the optimal one.

6. Conclusions

In this paper we studied the noise induced transitions between the two stable periodic orbits of the deterministic system. The method of action plot was employed to obtain the MPEP escaping across the unstable cycle, which is the minimizer of the action functional in the Freidlin–Wentzell large deviation theory. The prehistory probability distribution turned out to peak sharply along the MPEP and numerical and theoretic results showed good agreements. The action plot exhibited complicated and nested structures, with multiple local minima at the edges of hills. The mechanism of its formation was explained in detailed and various types of escaping trajectories are discussed.

Singularities are embodied in the existence of multiple local minima of the action functional. We then discussed its origins from a topological point of view, by considering structures of the Lagrangian manifold and action surface. The action surface has three sheets and the two lower ones intersect at a nonzero angle, giving rise to the switching line. The MPEP be-

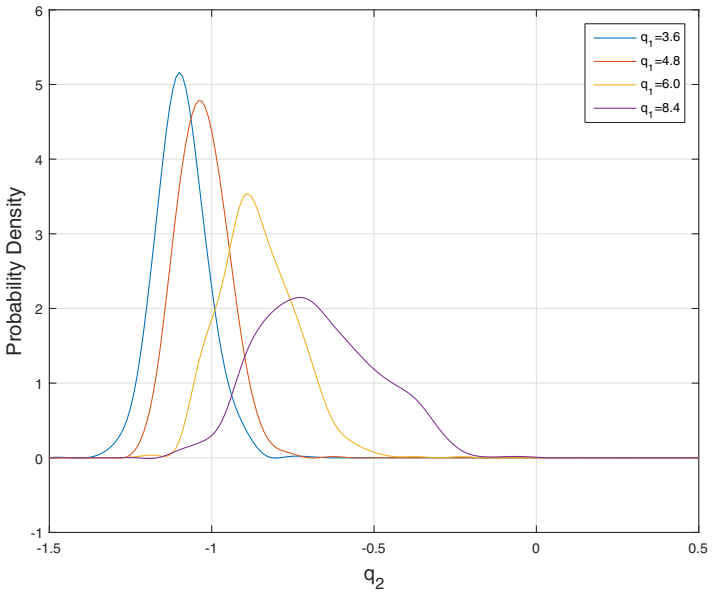

Fig. 8. Cross sections of the prehistory probability distribution of paths fluctuating to the cusp point with $q_{1f} = 9.2174$.

comes invalid when the end point is selected on the switching line since the prehistory distribution peaks along two paths, actions of which are almost equal. The cusp point is observed to have the effect of broadening the prehistory distribution of paths through it and the structure of action surface may provide a proper explanation. Therefore both the switching line and cusp point is of physical significance since they may have a particular impact on the MPEP and prehistory distributions.

Acknowledgments

This work was supported by the National Natural Science Foundation of China (No.11472126, 11232007), the Research Fund of State Key Laboratory of Mechanics and Control of Mechanical Structures (Nanjing University of Aeronautics and Astronautics) (Grant No.MCMS-0116G01).

References

[1] Freidlin MI, Wentzell AD. Random perturbations of dynamical systems.. Springer-Verlag; 2002.
[2] Grassberger P. Noise-induced escape from attractors. J Phys A Mathe Gen 1989;22(16):3283–90.
[3] Smelyanskiy VN, Dykman MI, Maier RS. Topological features of large fluctuations to the interior of a limit cycle. Phys Rev E 1997;55(3):2369–91.
[4] Luchinsky DG, Maier RS, Mannella R, Mcclintock PVE, Stein DL. Experiments on critical phenomena in a noisy exit problem. Phys Rev Lett 1997;79(17):3109–12.
[5] Kraut S, Grebogi C. Escaping from nonhyperbolic chaotic attractors. Phys Rev Lett 2004;92(23):1773–87.
[6] Chen Z, Li Y, Liu X. Noise induced escape from a nonhyperbolic chaotic attractor of a periodically driven nonlinear oscillator. Chaos 2016;26(6):935–92.
[7] Anishchenko VS, Khovanov IA, Khovanov NA, Luchinsky DG, McClintock PVE. Noise induced escape from the lorenz attractor. Fluctuation Noise Lett 2001;9(1):27–33.
[8] Zhou X, Weinan E. Study of noise-induced transitions in the lorenz system using the minimum action method. Commun Math Sci 2010;8(2):341–55.
[9] Dykman MI, Millonas MM, Smelyanskiy VN. Observable and hidden singular features of large fluctuations in nonequilibrium systems. Phys Lett A 1994;195(1):53–8.
[10] Dykman MI, Luchinsky DG, Mcclintock PV, Smelyanskiy VN. Corrals and critical behavior of the distribution of fluctuational paths. Phys Rev Lett 1997;77(26):5229–32.
[11] Chen Z, Liu X. Patterns and singular features of extreme fluctuational paths of a periodically driven system. Phys Lett A 2016;380(22–23):1953–8.
[12] Maier RS, Stein DL. Effect of focusing and caustics on exit phenomena in systems lacking detailed balance. Phys Rev Lett 1993;71(12):1783–6.
[13] Chen Z, Liu X. Singularities of fluctuational paths for an overdamped two-well system driven by white noise. Physica A Stat Mech Appl 2016;469(C):206–15.
[14] Dykman MI, Smelyanskiy VN, Luchinsky DG, Mannella R, McClintock PVE, Stein ND. Large fluctuations in a periodically driven dynamical system. Int J Bifurcation Chaos 1998;8(4):747–54.
[15] Graham R, Tl T. Existence of a potential for dissipative dynamical systems. Phys Rev Lett 1984;52(1):9–12.
[16] Jung P. Periodically driven stochastic systems. Phys Rep 1993;234(4–5):175–295.
[17] Kim S, Reichl LE. Stochastic chaos and resonance in a bistable stochastic system. Phys Rev E 1996;53(4):3088–95.
[18] Dykman MI, McClintock PVE, Smelyanski VN, Stein ND, Stocks NG. Optimal paths and the prehistory problem for large fluctuations in noise-driven systems. Phys Rev Lett 1992;68(18):2718.
[19] Luchinsky DG, Mcclintock PVE. Irreversibility of classical fluctuations studied in analogue electrical circuits. Nature 1997;389(6650):463–6.
[20] Whitney H. On singularities of mappings of euclidean spaces. i. mappings of the plane into the plane. Ann Math 1955;62(3):374–410.